www.nature.com/modpathol

ARTICLE

Sweat-gland carcinoma with neuroendocrine differentiation (SCAND): a clinicopathologic study of 13 cases with genetic analysis

Keisuke Goto[1,2,3,4,5,6]✉, Yoji Kukita[7], Keiichiro Honma[1], Nobuyuki Ohike[4], Takaya Komori[8], Yoshihiro Ishida[8], Misawo Ishikawa[9], Takashi Nakatsuka[10], Soichi Fumita[11], Koichi Nakagawa[12], Aya Okabayashi[13], Yoshifumi Iwahashi[14], Tomoyuki Tanino[15], Keisuke Kikuchi[16], Yoshie Kawahara[17], Tsunekazu Hishima[2], Jiro Uehara[18], Takuma Oishi[4] and Taiki Isei[19]

Low-grade neuroendocrine carcinoma of the skin (LGNECS) was proposed in 2017 as a new primary cutaneous neoplasm with neuroendocrine differentiation; however, it is not yet well known due to its rarity. Herein, we perform a detailed clinicopathologic analysis of 13 cases as well as panel DNA sequencing in three cases. The study included 12 males and 1 female with a median age of 71 (43–85) years. All lesions occurred on the ventral trunk. The mean tumor size was 2.2 (0.8–11.0) cm. The histopathology resembled that of well-differentiated neuroendocrine tumors (NETs) in other organs, but intraepidermal pagetoid spreading was seen in 8 (61.5%) cases and stromal mucin deposits in 4 (30.8%). Immunoreactivity for CK7, CK19, EMA, BerEP4, CEA, chromogranin A, synaptophysin, INSM1, GCDFP15, GATA3, ER, and bcl-2 were present in varying degrees in all tested cases. *PTEN* c.165-1G>A splice site mutation was detected by panel sequencing in one case, and *GATA3* P409fs*99 and *SETD2* R1708fs*4 in another case. Lymph node metastasis was seen significantly in cases with tumor size >2.0 cm [8/8 (100%) vs. 1/5 (20%)]. All three cases with size >3.0 cm were in unresectable advanced-stage [3/3 (100%) vs. 1/10 (10%)], and two of the three patients succumbed to the disease. The two cases of death revealed mild nuclear atypia (mitosis: 1/10 HPFs) and moderate nuclear atypia (2/10 HPFs). Thus, tumor size would be a better prognostic factor than nuclear atypia, mitotic count, and Ki67 index, unlike in NETs. These clinicopathologic and immunohistochemical features would represent the characteristics as skin adnexal tumors with apocrine/eccrine differentiation rather than NETs; therefore, we rename it as sweat-gland carcinoma with neuroendocrine differentiation (SCAND).

Modern Pathology (2022) 35:33–43; https://doi.org/10.1038/s41379-021-00921-8

INTRODUCTION

In the skin, Merkel cell carcinoma and endocrine mucin-producing sweat-gland carcinoma (EMPSGC) have been well established as primary cutaneous neoplasms with neuroendocrine differentiation. Merkel cell carcinoma, also known as primary cutaneous neuroendocrine carcinoma, is strongly associated with both sunlight exposure and Merkel cell polyomavirus infection[1]. The median age of the patients is 75 years, and 95% of the cases afflicted are Caucasian patients in the United States[2]. This tumor type exhibits a poor prognosis; the 5-year overall survival rates for patients with localized disease are estimated to be 51%, 35% for patients with regional metastasis, and 14% for patients with distant metastasis[3]. In contrast, EMPSGC is predominantly seen in females, and all reported cases were limited in the periorbital area[4–10]. This tumor type shows in situ growth or expanding invasion growth but does not show metastasis[10]. EMPSGC can be associated with neuroendocrine type mucinous carcinoma; thus, both would exist on the same spectrum[5,10].

Low-grade neuroendocrine carcinoma of the skin (LGNECS) was proposed in 2017 as a distinct third entity of primary cutaneous tumor with neuroendocrine differentiation[11]. LGNECS is cytologically low-grade and shows a different immunohistochemical profile from Merkel cell carcinoma. Unlike EMPSGC, LGNECS is an infiltrative tumor that is seen on the trunk but not on the face. However, there is scarcity of data about this skin tumor due to limited reports[11–13]. Herein, we performed a clinicopathologic and

[1]Department of Diagnostic Pathology and Cytology, Osaka International Cancer Institute, Osaka, Japan. [2]Department of Pathology, Tokyo Metropolitan Cancer and Infectious Disease Center Komagome Hospital, Tokyo, Japan. [3]Department of Pathology, Itabashi Central Clinical Laboratory, Tokyo, Japan. [4]Department of Diagnostic Pathology, Shizuoka Cancer Center Hospital, Sunto, Japan. [5]Department of Diagnostic Pathology, Osaka National Hospital, Osaka, Japan. [6]Department of Dermatology, Hyogo Cancer Center, Akashi, Japan. [7]Laboratory of Genomic Pathology, Research Center, Osaka International Cancer Institute, Osaka, Japan. [8]Department of Dermatology, Kyoto University Graduate School of Medicine, Kyoto, Japan. [9]Department of Diagnostic Pathology, Kainan Hospital, Yatomi, Japan. [10]Department of Plastic Surgery, JR Tokyo General Hospital, Tokyo, Japan. [11]Department of Medical Oncology, Kindai University, Osakasayama, Japan. [12]Department of Dermatology, Saiseikai Tondabayashi Hospital, Tondabayashi, Japan. [13]Department of Dermatology, Izumi City General Hospital, Izumi, Japan. [14]Department of Human Pathology and Diagnostic Pathology, Wakayama Medical University, Wakayama, Japan. [15]Department of Diagnostic Pathology, Tokyo Metropolitan Police Hospital, Tokyo, Japan. [16]Department of Diagnostic Pathology, Obihiro Kosei Hospital, Obihiro, Japan. [17]Department of Dermatology, Keiyu Hospital, Yokohama, Japan. [18]Department of Dermatologic Oncology, Tokyo Metropolitan Cancer and Infectious Disease Center Komagome Hospital, Tokyo, Japan. [19]Department of Dermatologic Oncology, Osaka International Cancer Institute, Osaka, Japan. ✉email: goto.keisuke@icloud.com

Received: 1 April 2021 Revised: 18 August 2021 Accepted: 20 August 2021
Published online: 12 September 2021

immunohistochemical analysis on 13 cases with this tumor as well as panel DNA sequencing in three cases, and investigated the prognostic factors.

MATERIALS/SUBJECTS AND METHODS

Case selection and clinical data

A total of 13 cases (cases 1–13) were retrieved from 11 institutes in which the authors served (2004 to 2020). Four cases (cases 1–3, 5) had been previously investigated in other studies[11,13] and were reevaluated in this study. Clinical data were extracted from medical records by referring clinicians and pathologists (Table 1). In all 13 cases, systemic examinations, including contrast-enhanced computed tomography (case 1–7, 9–13), non-contrast computed tomography (case 8), magnetic resonance imaging (cases 1, 3, 6, 7, 10, 12, 13), positron emission tomography-computed tomography (cases 3, 6, 10, 12, 13), gallium scintigraphy (cases 4, 13), gastrointestinal endoscopy and colonoscopy (cases 1, 2, 3, 5, 6, 12), cystoscopy (cases 2, 5), nasopharyngolaryngoscopy (case 12), mammary ultrasonography (cases 1, 10, 13), mammography (cases 1, 8, 13), and mastectomy (case 1), were performed to rule out the tumor origins from other organs.

The statistical associations of clinical outcomes were analyzed using Pearson's chi-square test. A two-tailed P value of <0.05 was considered statistically significant.

Histopathologic analysis

Hematoxylin–eosin and immunohistochemical staining were performed on 4-μm thick sections obtained from formalin-fixed paraffin-embedded (FFPE) tissues.

Histopathologically, nuclear atypia, mitotic count per 10 high-power fields (10 HPFs), involvement of subcutis, lymphatic invasion, histopathologic classification of carcinoid tumors (divided into three patterns: nodular solid nested pattern, trabecular or ribbon-like pattern, and tubular, acinar, or rosette-like pattern), intraepidermal pagetoid spreading of tumor cells, intraductal tumor component, and stromal mucin deposits were evaluated (Table 2).

Immunohistochemical analysis

Ventana BenchMark ULTRA system (Roche Diagnostics, Tucson, AZ, USA) was used with Ventana iView DAB IHC Detection Kit (Roche Diagnostics) or Ventana OptiView DAB IHC Detection Kit (Roche Diagnostics). The antibodies used in this study are listed in Table 3.

Reactions that labeled at least 1% of the tumor cells were considered positive; positivity was either rare (1–10%), focal (11–50%), partial (51–80%), or diffuse (81–100%). Staining intensity was graded as negative, weak, moderate, or strong. When the intensity was heterogeneous, the predominant intensity was recorded.

Regarding HER2 and somatostatin receptor subtype 2a (SSTR2), the immunoreactivity was estimated using HER2 and SSTR2 scoring systems[14], respectively. The staining of p53 was evaluated for wild (heterogeneous) or mutant type (diffuse strong or null) positivity. PTEN and Rb expressions were checked for complete or partial loss. Ki67 labeling index was determined by counting 1000 cancer cells within hot spots in each case.

Next generation sequencing analysis

In three cases (cases 6, 7, and 12), DNA was extracted from FFPE tissues using QIAamp DNA FFPE Tissue Kit (Qiagen, Hilden, Germany) or Maxwell® RSC DNA FFPE Kit (Promega, Madison, WI, USA). Targeted DNA sequencing was performed using Ion AmpliSeq™ Cancer Hotspot Panel v2 (Thermo Fisher Scientific, Waltham, MA, USA) by Macrogen Japan (Tokyo, Japan) for cases 6 and 7 and FoundationOne CDx (Foundation Medicine, Inc., Cambridge, MA, USA) for case 12. The former panel surveys the hotspot regions of ~2800 mutations from 50 genes, and the latter panel does various types of genetic alterations in 324 genes.

Table 1. Clinical data in all cases of this study.

	Age (y)	Sex	Location	Size (cm)	Preop duration	Follow-up duration	Metastasis	Treatment and clinical outcome	Serum tumor markers
1	73	F	Anterior chest	0.8	1 y	7 y	No	NED after CEx (mastectomy) and LND	ND
2	72	M	Anterior chest	2.0	4–5 y	5 y	No	NED after CEx (no SLN biopsy)	ND
3	73	M	Inguinal region	11.0	>20 y	4 y 9 mo	RLN, hilar LN, bones, adrenal glands and peritoneum	Tumor death after palliative resection, LND and pharmacotherapy[a] (PD)	NSE 9.92 ng/mL
4	85	M	Inguinal region	4.0	5 y	2 y 5 mo	RLN and paraaortic LN	LN swelling after palliative resection, LND, RT, and avelumab (SD)	CEA 3.1 ng/mL, CA19-9 5.5 U/mL
5	61	M	Navel	3.5	3 y	5 y 2 mo	RLN, axillary LN, lungs, peritoneum, bones	Tumor death after CEx, LN biopsy, everolimus (SD), octreotide (SD) and RT	ND
6	68	M	Pubic region	1.7	3 y	1 y	RLN	NED after CEx, LND, RT, tamoxifen and paclitaxel	CA15–3 17.3 U/mL, NSE 14.6 ng/mL
7	67	M	Anterior chest	2.2	1 y	15 y	RLN, mediastinal LN, bones, lungs, pleura	Paclitaxel (PR) for a recurrence with systemic metastases in 13 y after CEx and LND (CA15–3 700.6 U/mL, NSE 15.5 ng/mL)	CA15–3 1216.6 U/mL, NSE 102.5 ng/mL, CYFRA 23.5 ng/mL (recurrent)
8	53	M	Pubic region	1.0	A few y	1 y 4 mo	No	NED after CEx (no SLN biopsy)	CEA 2.1 ng/mL, CA19-9 6.3 U/mL
9	72	M	Anterior chest	2.5	2 y	1 y	RLN	Local recurrence and RLN metastasis after CEx	ND
10	43	M	Anterior chest	2.6	2 y	1 y	RLN	NED after CEx, LND and RT	ND
11	71	M	Anterior chest	1.7	8 mo	1 y	No	NED after CEx and SLN biopsy	CA15–3 17.0 U/mL
12	80	M	Inguinal region	2.2	5 y	7 mo	RLN	NED after CEx and LND	CEA 18.6 ng/mL
13	67	M	Anterior chest	2.0	ND	5 y 2 mo	RLN	NED after CEx and LND	ND

CA15–3 carbohydrate antigen 15–3 (normal range <25 U/mL), *CA19-9* carbohydrate antigen 19-9 (normal range <37 U/mL), *CEA* carcinoembryonic antigen (normal range <5 ng/mL), *CEx* complete excision, *CYFRA* cytokeratin 19 fragment (normal range <2.8 ng/mL), *F* female, *LN* lymph node, *LND* lymph node dissection, *M* male, *mo* month(s), *ND* not described, *NED* no evidence of disease, *NSE* neuron-specific nolase (normal range <12.0 ng/mL), *PD* progressive disease, *PR* partial response, *RLN* regional lymph node, *RT* radiotherapy, *SD* stable disease, *SLN* sentinel lymph node, *y* year(s).
[a]Etoposide and cisplatin (first line), amurubicin (second line), irinotecan (third line), doxorubicin and cyclophosphamide (fourth line), etoposide (fifth line), and avelumab (sixth line).

Table 2. Histopathologic findings and Ki67 labeling index in all cases of this study.

	Atypia	Mitosis (/10 HPFs)	Ki67 LI	Involvement of subcutis	LyI	Histopathologic pattern (%)	Pagetoid spread	IDC	Mucin deposit (%)
1	Mild	1	6.5%	No	No	NS (90), TR (10)	No	Yes	No
2	Mild	1	14.0%	Yes	No	NS (100)	Yes	Yes	No
3	Moderate	2	14.7%	Yes	Yes	NS (95), TR (5)	Yes	Yes	No
4	Severe	13	14.5%	Yes	Yes	NS (40), TR (50), TU (10)	Yes	Yes	Yes (25)
5	Mild	1	8.5%	Yes	Yes	NS (80), TR (15), TU (5)	Yes	Yes	Yes (5)
6	Moderate	5	15.7%	Yes	Yes	NS (50), TR (25), TU (25)	Yes	Yes	No
7	Mild	1	3.5%	Yes	Yes	NS (100)	Yes	Yes	No
8	Mild	0	8.8%	Yes	No	NS (5), TU (95)	No	No	No
9	Severe	32	62.4%	Yes	No	NS (100)	No	No	No
10	Severe	17	13.6%	Yes	Yes	NS (75), TR (5), TU (20)	Yes	Yes	Yes (10)
11	Mild	2	7.5%	Yes	No	NS (30), TU (70)	No	No	No
12	Moderate	14	24.0%	Yes	Yes	NS (90), TR (5), TU (5)	Yes	Yes	Yes (10)
13	Moderate	16	10.4%	Yes	Yes	NS (100)	No	No	No

HPF high-power field, *IDC* intraductal tumor component, *LI* labeling index, *LyI* lymphatic invasion, *NS* nodular solid nested pattern, *TR* trabecular or ribbon-like pattern, *TU* tubular, acinar, or rosette-like pattern.

To remove polymorphic variants, we used information of allele frequencies (AFs) in public polymorphic variants databases, and excluded any variants with an observed AF ≥ 0.5% in any of ethnic populations in gnomAD exome (v2.0.1), gnomAD genome (v2.0.1)[15], 1000 genomes (2015 August collection)[16], NHLBI Exome Sequencing Project with 6500 exomes (https://evs.gs.washington.edu/EVS/), and two Japanese databases: 4.7KJPN Allele Frequency Panel (v20190826)[17] and HGVD (v2.30)[18], with ANNOVAR[19]. Pathogenicity of variant (≥5% variant allele fraction) was evaluated using information from variant catalogs, COSMIC (https://cancer.sanger.ac.uk/cosmic), OncoKB (https://www.oncokb.org/), and ClinVar (https://www.ncbi.nlm.nih.gov/clinvar/).

RESULTS

Clinical findings and courses

The clinical features of the 13 patients included in this study are summarized in Table 1. The clinical pictures of cases 2, 3, 5, 6, 8, and 11 are presented in Fig. 1.

The patients included 12 males and 1 female with a median age at diagnosis of 71 years (range: 43–85 years). The tumor locations were the anterior chest (breast or presternal region) ($n = 7$), navel ($n = 1$), pubic region ($n = 2$), and inguinal regions ($n = 3$), all of which are located on or close to the milk-lines on the trunk. The average size of the tumors was 2.2 cm (range: 0.8–11.0 cm). Macroscopically, early lesions demonstrated erythema with induration, a papule, or both (Fig. 1A–C). Advanced lesions presented an elevated nodule with a mulberry-like surface appearance (Fig. 1D–F). No mammary tumor was clinically confirmed in all cases.

Follow-up data were available for all 13 cases, ranging from 7 months to 15 years (median 2 years and 5 months). Of the 13 cases, 9 cases (cases 3–7, 9, 10, 12, 13) (69.2%) exhibited regional lymph node metastasis and 4 (cases 3–5, 7) (30.8%) showed non-regional lymph node metastasis as well. Three cases (cases 3, 5, 7) (23.1%) presented with distant metastasis or dissemination to the peritoneum (cases 3 and 5), pleura (case 7), lung (cases 5, 7), adrenal gland (case 3), or bone (cases 3, 5, 7). One patient (case 7) experienced a recurrence with distant metastasis after 13 years, in which partial response was achieved with weekly paclitaxel therapy.

All eight cases with maximum tumor size >2.0 cm exhibited lymph node metastasis, while only one of the other five cases with tumor size ≤2.0 cm did [8/8 (100%) vs. 1/5 (20.0%); $P = 0.0024$]. All three cases with tumor size >3.0 cm were in unresectable advanced stages, although only one of ten cases with tumor size ≤3.0 cm was in an unresectable advanced-stage [3/3 (100%) vs. 1/10 (10%); $P = 0.003$]. Moreover, two of the three patients succumbed to the disease [2/3 (66.7%) vs. 0/10 (0%); $P = 0.005$].

Histopathologic findings

The histopathologic features are shown in Figs. 2, 3 and summarized in Table 2.

All tumors occurred in the dermis, and 12 (92.3%) of the 13 lesions involved the subcutis; however, there was no tumor associated with mammary glands or ducts. All of them, including early small-sized tumors, presented a poorly circumscribed margin with an infiltrating growth, while five (cases 3, 4, 7, 9, 10) (38.5%) of 13 cases exhibited a well-circumscribed pushing margin in the subcutaneous deep area (Fig. 2). No apparent differentiation toward apocrine or eccrine apparatus (e.g., apocrine snouts) was seen in all tumors. The three classic cell arrangements, nodular/solid/nested pattern, trabecular/ribbon-like pattern, tubular/acinar/rosette-like pattern, were observed in varying proportions. Tumor cell aggregations that varied greatly in size and shape had abundant capillary networks around and within the tumor nests. The tumor cells contained round to oval nuclei with coarse granular chromatin and relatively inconspicuous nucleoli and fine eosinophilic granular cytoplasm. Focal pagetoid extension of the tumor cells within the overlying epidermis was observed in eight (61.5%) cases (Fig. 3D). Limited tumor component in the eccrine apparatus were seen in nine (69.2%) cases (Fig. 3E). Four (30.8%) cases exhibited stromal mucin deposits in limited areas (≤25% of the tumor area) (Fig. 3F). Nuclear atypia and mitotic counts per 10 HPFs (×40 objective and eyepiece of field number 22) were mild [median 1 (0–2)/10 HPFs] ($n = 6$), moderate [9.5 (2–16)/10 HPFs] ($n = 4$), and severe [17 (13–32)/10 HPFs] ($n = 3$), respectively (Fig. 4). In cases 3 and 5 associated with tumor-related death, moderate nuclear atypia (mitosis: 2/10 HPFs) and mild nuclear atypia (mitosis: 1/10 HPFs) was seen, respectively.

Immunohistochemical findings

The immunohistochemical findings of the 13 cases are summarized in Table 4 and shown in Fig. 5.

In all evaluated cases, tumor cells were positive for pan-cytokeratin (AE1/AE3, CAM5.2), cytokeratin 7, cytokeratin 19,

Table 3. The immunohistochemical antibodies used in this study.

	Clone	Dilution	Source
Androgen receptor	SP107	Prediluted	Roche Diagnostics, Tucson, AZ, USA
Bcl-2	SP66	Prediluted	Roche Diagnostics
BerEP4	BerEP4	Prediluted	Roche Diagnostics
c-KIT	9.7	Prediluted	Roche Diagnostics
Carbohydrate antigen 125	M11	1:800	Dako, Glostrup, Denmark
Carbohydrate antigen 19-9	121SLE	Prediluted	Roche Diagnostics
Carcinoembryonic antigen	CEA31	Prediluted	Roche Diagnostics
CD56	MRQ-42	Prediluted	Roche Diagnostics
CDX2	EPR2764Y	Prediluted	Roche Diagnostics
Chromogranin A	LK2H10	Prediluted	Roche Diagnostics
Cytokeratin 5/6	DE-K13	1:50	Dako
Cytokeratin 7	SP52	Prediluted	Roche Diagnostics
Cytokeratin 19	A53B/A2.26	Prediluted	Roche Diagnostics
Cytokeratin 20	SP33	Prediluted	Roche Diagnostics
Cytokeratin AE1/AE3	AE1/AE3 & PCK26	Prediluted	Roche Diagnostics
Cytokeratin CAM5.2	CAM5.2	Prediluted	Roche Diagnostics
Epithelial membrane antigen	E29	Prediluted	Roche Diagnostics
Estrogen receptor	SP1	Prediluted	Roche Diagnostics
GATA3	L50-823	Prediluted	Roche Diagnostics
Gross cystic disease fluid protein 15	EP1582Y	Prediluted	Roche Diagnostics
HER2	4B5	Prediluted	Roche Diagnostics
Insulinoma-associated protein 1	A-8	1:100	Santa Cruz Biotechnology, Santa Cruz, CA, USA
Ki67	MIB-1	1:500	Dako
Mammaglobin	31A5	Prediluted	Roche Diagnostics
Merkel cell polyomavirus large T antigen	CM2B4	1:50	Santa Cruz Biotechnology
MUC1	H23	Prediluted	Roche Diagnostics
MUC2	MRQ-18	Prediluted	Roche Diagnostics
MUC5AC	MRQ-19	Prediluted	Roche Diagnostics
MUC6	MRQ-20	Prediluted	Roche Diagnostics
Neurofilament	2F11	1:5	Dako
p16	E6H4	Prediluted	Roche Diagnostics
p53	DO-7	Prediluted	Roche Diagnostics
p63	4A4	Prediluted	Roche Diagnostics
Progesterone receptor	1E2	Prediluted	Roche Diagnostics
PTEN	138G6	1:100	Cell Signaling Technology, Danvers, MA, USA
Rb	G3-245	1:100	BD Biosciences, San Diego, CA, USA
S100 protein	Polyclonal	Prediluted	Roche Diagnostics
Somatostatin receptor subtype 2a	EP149	Prediluted	Nichirei Bioscience, Tokyo, Japan
SOX10	SP267	Prediluted	Roche Diagnostics
Synaptophysin	MRQ-40	Prediluted	Roche Diagnostics
TTF1	8G7G3	Prediluted	Dako

carcinoembryonic antigen (CEA), epithelial membranous antigen (EMA), MUC1, MUC5AC, BerEP4, CEA, chromogranin A, synaptophysin, insulinoma-associated protein 1 (INSM1), gross cystic disease fluid protein 15 (GCDFP15), GATA3, estrogen receptor (ER), progesterone receptor (PgR), p16, and bcl-2, but completely negative for cytokeratin 5/6, cytokeratin 20, p63, carbohydrate antigen 19-9 (CA19-9), carbohydrate antigen 125 (CA125), neurofilament, Merkel cell polyomavirus large T antigen, c-KIT, S100 protein, SOX10, CDX2, and TTF1 (Table 4). Some cases exhibited immunoreactivity for MUC2, MUC6, CD56, androgen receptor, and mammaglobin. Paranuclear dot-like staining was not observed in any cytokeratin markers.

The HER2 score was 0 ($n = 8$) or 1+ ($n = 5$) in all 13 cases. SSTR2 score was 0 ($n = 2$, cases 4, 12), 1 ($n = 1$; case 11), 2 ($n = 5$; cases 3, 5, 6, 8, 9), or 3 ($n = 1$; case 2). A mutant pattern of diffuse and strong immunoreactivity for p53 was seen in only one lesion (case 13), but a wild-type pattern was observed in the other eight evaluated tumors (cases 1, 2, 4, 6, 8–10, 12). Complete loss of PTEN immunoexpression was seen in 1 case (cases 7) and partial loss was in 1 case (case 5). The other 11 cases exhibited preserved expression of PTEN. Rb immunoexpression was intact in all evaluated cases ($n = 7$; cases 2–4, 6, 8, 9, 12).

The median labeling index of Ki67 was 13.6% (range: 3.5–62.4%). No case showed a Ki67 labeling index less than 2%

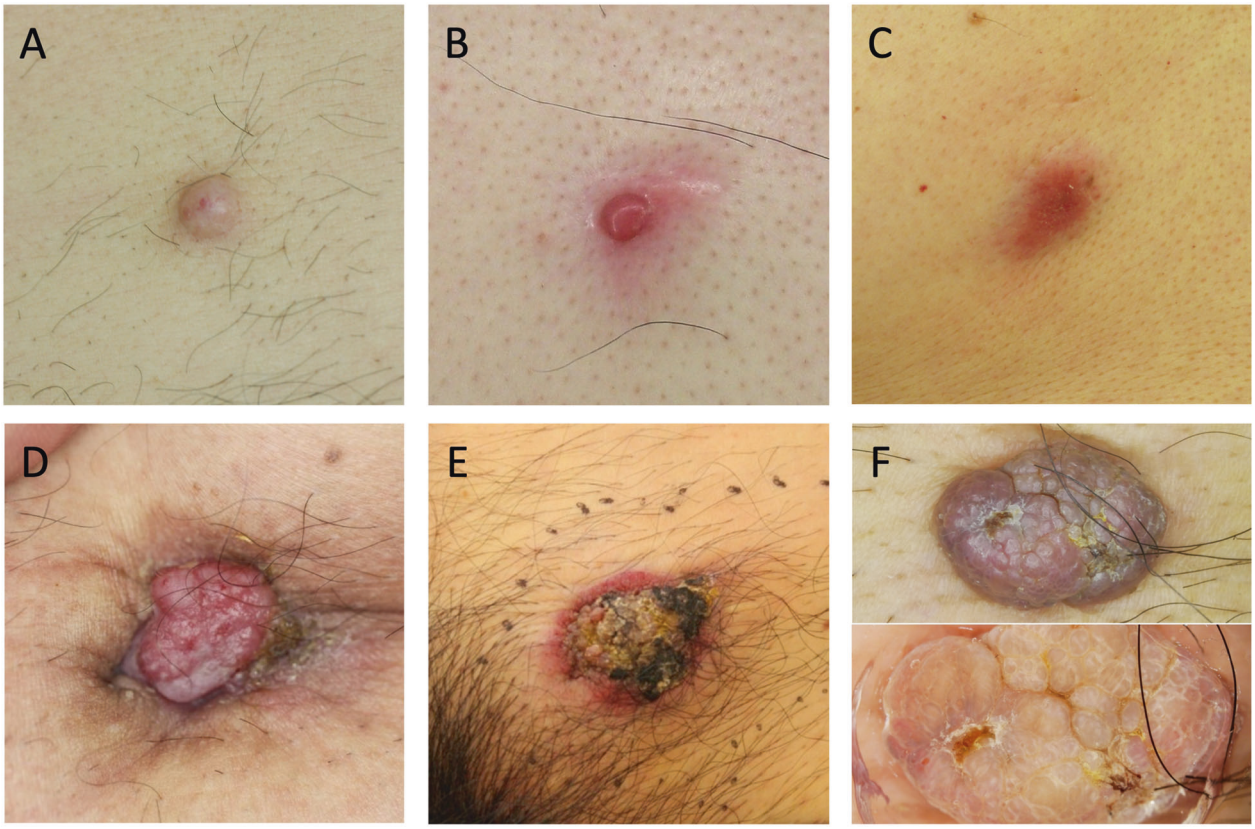

Fig. 1 Clinical findings of sweat-gland carcinoma with neuroendocrine differentiation (SCAND)/low-grade neuroendocrine carcinoma of the skin (LGNECS). Early lesions were pink or reddish and seen as a nodule (**A** case 8), a nodule within an induration (**B** case 2), or an induration (**C** case 11). Advanced lesions showed a reddish irregular-shaped tumor with mulberry-like surface (**D** case 5), sometimes with crust formation (**E** case 3). Mulberry-like surface was clear in dermoscopic examination (**F** case 6).

and only 2 cases (cases 9 and 12) showed an index more than 20%. In cases with lymph node metastasis ($n = 9$), the Ki67 labeling index was 8.8% (6.5–62.4%), while the index in cases without lymph node metastasis ($n = 4$) was 14.1% (3.5–24.0%). The Ki67 labeling index in cases showing distant metastasis ($n = 4$) was 8.5% (3.5–14.7%). Two cases with tumor-related death displayed Ki67 labeling index of 8.5% and 14.7%, respectively.

Next generation sequencing

A total of nine mutations, including 1 mutation of *PTEN*, 2 mutations of *PIK3CA*, and six mutations of *FLT3*, were revealed in case 7, but only *PTEN* c.165-1G>A splice site mutation was evaluated as a pathogenic one with reference to COSMIC and ClinVar. In case 12, *GATA3* P409fs*99 and *SETD2* R1708fs*4 were detected as pathogenic mutations. In contrast, no significant gene mutation was detected in case 6.

DISCUSSION

Until 2017, there had been 14 cases of primary cutaneous carcinoid tumors[20–32]. However, breast carcinoma[25], basal cell carcinoma[30,31], and trichoblastic tumors (trichoblastoma or basal cell carcinoma)[23] have been misdiagnosed as primary cutaneous carcinoid tumors in four literature cases. Moreover, five of the other ten cases were located on the scalp of females[20,27,29,32]. The scalp is a favorite site of skin metastasis[33,34]; therefore, the five cases may be metastatic NETs from other organs. While one case was seen on the back[28], the other four tumors were located close to the milk-line of three males and one female, all of which could be LGNECS[21,22,24,26]. In 2017, three cases were analyzed and labeled as LGNECS[11], and three additional cases were reported as LGNECS[12,13]. In addition, one case excluded from a study of high-grade neuroendocrine carcinoma of the vulva seemed to be LGNECS[35]. Our present study is the largest case series and would reveal several new clinical, histopathological, immunohistochemical, and molecular features of this tumor.

Several clinical characteristics of LGNECS were documented in this study. The prominent male predominance (12:1) in LGNECS was contrasting to the female predominance in EMPSGC[10]. All patients were middle-aged or elderly. The tumor locations of all 13 cases were the anterior chest, abdomen, and inguinal regions, all of which were in the anterior trunk close to or on milk-lines. No cases had tumors located on the head and neck, back, buttocks, and extremities in this study. The sites of predilection of LGNECS differ from that of EMPSGC (periorbital areas)[4–10] or Merkel cell carcinoma (sun-damaged areas)[1]. In spite of the tumor topography close to milk-lines, it is unlikely that the origin of LGNECS is associated with accessory mammary tissues because LGNECS was predominant in males and there was no case with axillary tumors or with the involvement of mammary glands in this study.

In the early phase, the lesion arises in the dermis and clinically appears as an erythematous induration, a nodule, or a combination. In the advanced phase, the lesion becomes a reddish tumor with a mulberry-like surface. This tumor often grows up in the dermis and subcutis; thus, the maximum tumor size would not be equivalent to the diameter of an exophytic tumor part.

The serum levels of carbohydrate antigen 15–3 and CEA were elevated in some advanced-stage cases, but not in early stage cases. These serum tumor markers do not seem to be very sensitive for diagnosis or follow-up.

LGNECS is not an indolent neoplasm, although cytologically low-grade. For prognosis prediction, tumor diameter may be a

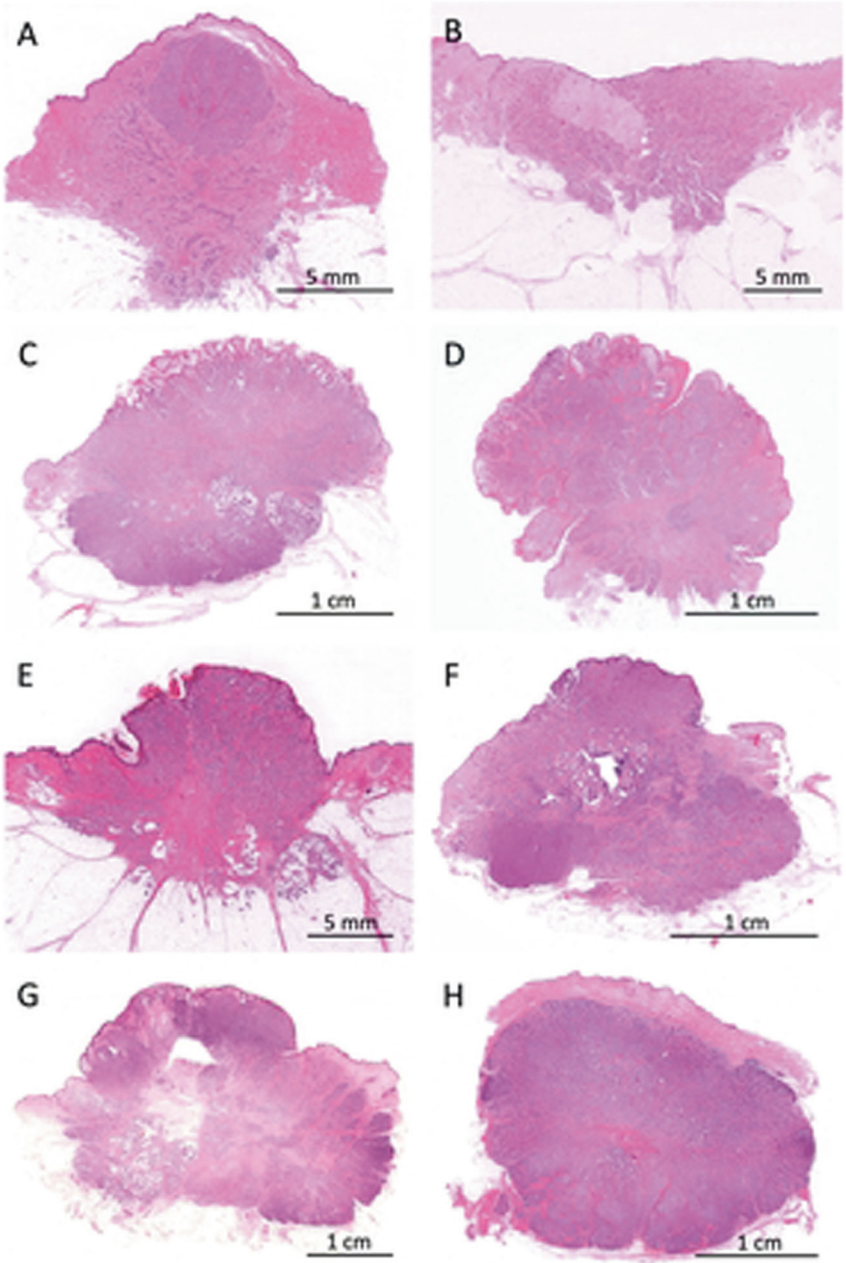

Fig. 2 Tumor silhouettes of sweat-gland carcinoma with neuroendocrine differentiation (SCAND)/low-grade neuroendocrine carcinoma of the skin (LGNECS). Early lesions presented as an infiltrative nodular tumor (**A** case 8) or an indurated tumor (**B** case 11) without epidermal changes. Advanced lesions involving an overlying epidermis usually showed a rough surface (**C** case 10; **D** case 12; **E** case 6; **F** case 7; **G** case 4), but rarely occurred in the deep dermis and did not involve an overlying epidermis (**H** case 9).

more reliable factor than nuclear atypia, mitotic count, and Ki67 labeling index, although case number in this study is small. Cases with a maximum tumor size >2.0 cm frequently (8/8, 100%) showed lymph node metastasis, and all 3 cases with a maximum tumor size >3.0 cm were in unresectable advanced stages (3/3, 100%). Moreover, 2 of the 3 patients died of the tumor. It should be noted that while measuring the maximum tumor size for prognosis prediction must be focused not only on the exophytic part of tumor but also on the deeper part. In the present study, mitotic count and Ki67 labeling index do not seem to be related to the prognosis; thus, grading system (G1–G3) based on mitotic count or Ki67 labeling index, similar to that in gastroenteropancreatic neuroendocrine tumors (GEP-NET), might not be necessary in LGNECS[36]. This may support that LGNECS is not in the NET category.

For treatment and management, complete surgical excision is essential, and sentinel lymph node biopsy should also be considered. There was one advanced-stage case (case 7) which responded to paclitaxel; thus, this could be one of the treatment options in unresectable cases. In addition, LGNECS may be responsive to selective ER modulators, including tamoxifen, because all cases in this study exhibited diffuse and strong immunoreactivity for ER. Therefore, drug therapies for breast cancer may be effective for LGNECS, although anti-HER2 therapy including pertuzumab and trastuzumab would not be expected. In some LGNECS cases, somatostatin analogues, such as octreotide,

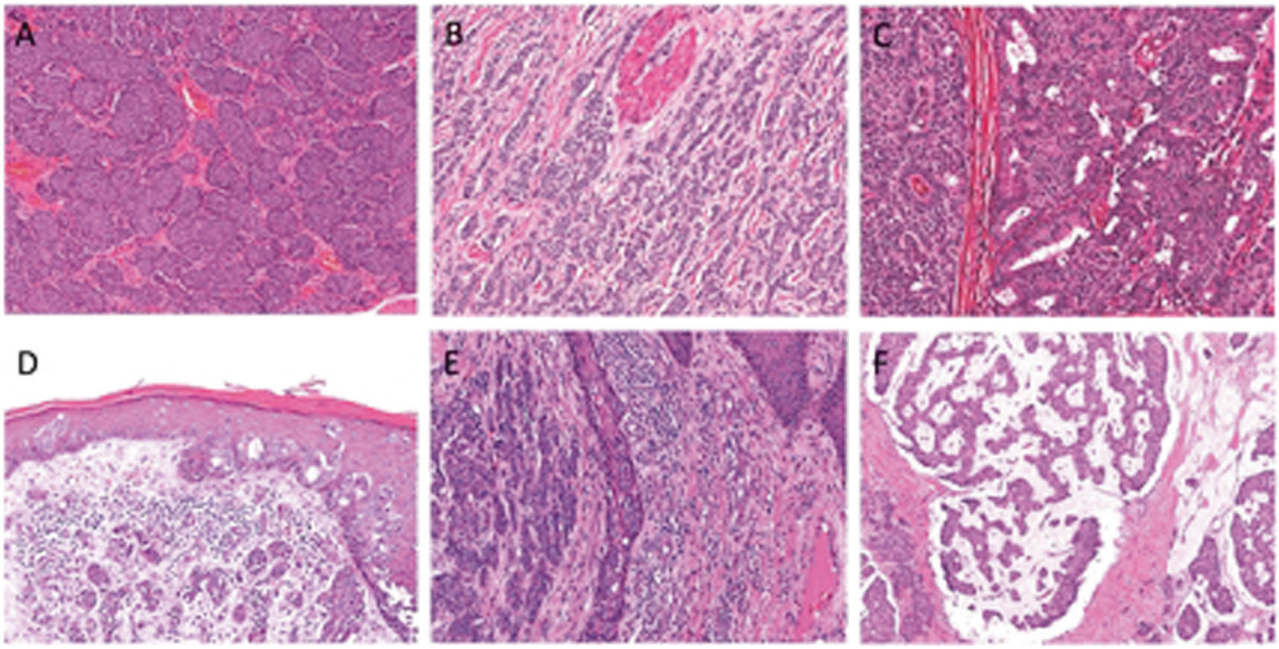

Fig. 3 Histopathologic findings of sweat-gland carcinoma with neuroendocrine differentiation (SCAND)/low-grade neuroendocrine carcinoma of the skin (LGNECS). Nodular solid nested pattern (**A** case 13), trabecular or ribbon-like pattern (**B** case 4), and tubular, acinar, or rosette-like pattern (**C** case 8) were observed in varying proportions. Intraepidermal pagetoid spreading of tumor cells was focally seen in eight tumors (**D** case 4). Intraductal tumor extension in eccrine apparatus was also observed in nine tumors (**E** case 5). Stromal mucin deposits were focally recognized in four lesions (**F** case 4).

may also be administered. Case 7 demonstrated recurrence with distant metastasis 13 years after initial remission; thus, long-term follow-up is necessary for patients with LGNECS.

The histopathological and cytological features of LGNECS were similar to those of NETs in other organs: various sizes and shapes of tumor nests, round to oval nuclei with coarse granular or salt-and-pepper chromatin and relatively inconspicuous nucleoli, relatively abundant cytoplasm with fine granules, abundant capillary network seen around and within tumor nests were observed. The tumor nests in NETs are classically divided into three patterns: nodular solid nested pattern, trabecular or ribbon-like pattern, and tubular, acinar, or rosette-like pattern[37]. LGNECS also showed these three patterns in various proportions. In contrast, epidermal hyperplasia with expanding papillary dermis (clinically corresponding to mulberry-like surface), intraepidermal or intraductal pagetoid spreading of tumor cells, and stromal mucin deposits were characteristic of LGNECS.

The immunoprofile in LGNECS was uniform in all cases in this study. Although immunoreactivity for MUC2, MUC6, CD56, androgen receptor, and mammaglobin was variable, expression of other markers was consistently positive or negative. Because LGNECS frequently expresses cytokeratin 7, cytokeratin 19, BerEP4, CEA, GCDFP15, GATA3, ER, and PgR, it is considered that this tumor originates from apocrine/eccrine apparatus and shows apocrine/eccrine differentiation. For distinguishing LGNECS from metastatic NETs to the skin, positivity for GCDFP15, GATA3, CEA, and ER and negativity for TTF1, CDX2, CA19-9, and CA125 may be helpful.

PTEN c.165-1G>A splice site mutation detected in case 7 was considered as a pathogenic alteration by database of COSMIC and ClinVar. It would be supported by the complete loss of PTEN immunoexpression in case 7. The gene of *PTEN* is a tumor suppressor gene located on human chromosome 10q23.3, encoding PTEN protein that regulates apoptosis, proliferation, survival, energy metabolism, cellular architecture, and motility by interfering with phosphoinositide-3 kinase/protein kinase B signaling[38]. The inactivation of PTEN is frequently seen in several cancers of various organs[39]. In addition, *PTEN* inactivating mutations have been so far reported in NETs of lung, pancreas, gastrointestinal tract, and uterine cervix, while the frequency is not high[40–45].

Differential diagnoses of LGNECS include EMPSGC, Merkel cell carcinoma, metastatic NET from other organs, breast carcinoma, Ewing sarcoma, in particular adamantinoma-like variant, basal cell carcinoma, sebaceoma, and several adnexal tumors with apocrine/eccrine differentiation. The location of the trunk and infiltrating growth pattern can rule out EMPSGC. The cytological features and immunoprofile of LGNECS are different from those of Merkel cell carcinoma. Immunohistochemistry would be helpful to differentiate LGNECS from other NETs, as described above. Breast carcinoma, especially solid-papillary carcinoma, is similar to LGNECS; however, male predominance, dermal tumor localization with no association with mammary glands, and lack of breast tumor can distinguish LGNECS from breast carcinoma. While solid-papillary carcinoma shows in situ or expansive and circumscribed growth, LGNECS is infiltrative even in early lesions. Adamantinoma-like Ewing sarcoma can be ruled out by the lack of p40/p63 immunoexpression and *EWSR1* rearrangement[46]. The histomorphology of LGNECS does not show pilosebaceous differentiation; thus, it is not difficult to distinguish LGNECS from basal cell carcinoma and sebaceoma. The absence of poroid cells and cuticular cells, positivity for neuroendocrine immunomarkers, and negativity for p40/p63 and c-KIT can rule out poroid neoplasms[47–49]. Apocrine carcinoma is characterized by apocrine gland differentiation (apocrine snouts and eosinophilic granular cytoplasm) and does not immunoexpress neuroendocrine markers, ER, and PgR.

LGNECS exhibited neither apparent apocrine gland differentiation (apocrine snouts and eosinophilic granular cytoplasm) nor eccrine gland differentiation (immunoexpression of c-KIT, S100 protein, and SOX10). However, the immunoexpression of other markers, including cytokeratin 19, BerEP4, GCDFP15, GATA3, ER, and PgR would suggest apocrine/eccrine sweat apparatus origin and differentiation; therefore, LGNECS could be a carcinoma with

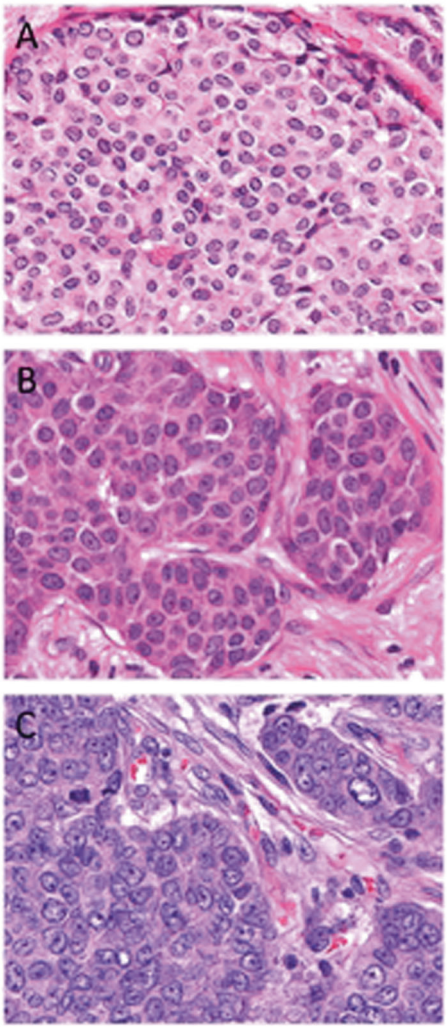

Fig. 4 Nuclear atypia of sweat-gland carcinoma with neuroendocrine differentiation (SCAND)/low-grade neuroendocrine carcinoma of the skin (LGNECS). Cytologically, nuclear atypia was graded into mild (**A** case 1), moderate (**B** case 6), and severe (**C** case 9). All images were obtained using ×10 (ocular) and ×60 (objective) lenses.

sweat-gland and neuroendocrine differentiation. In preexisting literature, there are three cases reported as cutaneous apocrine carcinoma with neuroendocrine differentiation (pubic region of a 79-year-old male, vulva of a 43-year-old female, pubic region of a 63-year-old male)[50–52]. In the articles, the three tumors do not show any definitive morphological findings of apocrine differentiation; thus, they could also be actually LGNECS.

In summary, LGNECS usually occurs in the anterior trunk, particularly close to or on milk-lines, of middle-aged to elderly males. Histopathology of LGNECS is similar to that of NETs in other organs, but papillomatous epidermal hyperplasia, intraepithelial pagetoid spreading of tumor cells, and stromal mucin deposits are characteristic of LGNECS. Diffuse immunoexpression of cytokeratin 19, EMA, MUC1, BerEP4, CEA, chromogranin A, synaptophysin, INSM1, GCDFP15, GATA3, ER, PgR, and bcl-2 are frequently observed in LGNECS. Lymph node metastasis was seen significantly in cases with a tumor size >2.0 cm. All three patients with a size >3.0 cm were in unresectable advanced stages, and two of the three patients died of the tumor. For LGNECS, tumor diameter would be a reliable prognostic factor, but nuclear atypia, mitotic counts, and Ki67 index would not, although the case number of our study is small. Complete surgical resection in the early stage (tumor size ≤2.0 cm) is recommended. For unresectable cases, paclitaxel and selective ER modulators may be effective. The somatostatin analog of octreotide can also be used in cases with overexpression of SSTR2.

The concept of LGNECS was expanded in this study. The clinicopathologic and immunohistochemical features could represent the characteristics of cutaneous adnexal tumors with apocrine/eccrine differentiation rather than NETs. The biological behavior is not indolent, whereas the cytology is usually low-grade.

Table 4. The immunohistochemical findings in this study.

	Positivity	Extent (number)	Intensity (number)
Cytokeratin AE1/AE3	3/3 (100%)	D (3)	S (3)
Cytokeratin CAM5.2	2/2 (100%)	D (2)	S (2)
Cytokeratin 5/6	0/4 (0%)		
Cytokeratin 7	13/13 (100%)	D (7), P (2), F (3), R (1)	S (6), M (4), W (3)
Cytokeratin 19	10/10 (100%)	D (10)	S (10)
Cytokeratin 20	0/12 (0%)		
p63	0/9 (0%)		
Epithelial membrane antigen	8/8 (100%)	D (8)	S (8)
MUC1	7/7 (100%)	D (6), P (1)	S (2), M (5)
MUC2	3/6 (50%)	F (1), R (2)	S (2), W (1)
MUC5AC	6/6 (100%)	D (2), P (2), F (2)	W (6)
MUC6	1/6 (17%)	F (1)	M (1)
BerEP4	11/11 (100%)	D (11)	S (10), M (1)
Carcinoembryonic antigen	13/13 (100%)	D (12), P (1)	S (13)
CA19-9	0/3 (0%)		
CA125	0/1 (0%)		
CD56	9/12 (75%)	D (3), P (1), F (3), R (2)	S (2), M (5), W (2)
Chromogranin A	12/12 (100%)	D (8), P (2), F (2)	S (6), M (6)
Synaptophysin	12/12 (100%)	D (10), F (2)	S (8), M (3), W (1)
Insulinoma-associated protein 1	13/13 (100%)	D (10), P (2), R (1)	S (10), M (3)
GCDFP15	13/13 (100%)	D (7), P (3), F (2), R (1)	S (6), M (4), W (3)
Mammaglobin	7/11 (64%)	F* (7)	S (6), M (1)
GATA3	12/12 (100%)	D (12)	S (12)
Estrogen receptor	13/13 (100%)	D (13)	S (12), M (1)
Progesterone receptor	13/13 (100%)	D (13)	S (12), M (1)
Androgen receptor	3/9 (33%)	D (1), P (1), R (1)	M (3)
Merkel cell polyomavirus large T antigen	0/11 (0%)		
Neurofilament	0/7 (0%)		
c-KIT	0/7 (0%)		
Bcl-2	11/11 (100%)	D (11)	S (11)
S100 protein	0/3 (0%)		
SOX10	0/3 (0%)		
TTF1	0/8 (0%)		
CDX2	0/6 (0%)		
p16	8/8 (100%)	D (1), P* (3), F* (4)	S (1), M (6), W (1)

D diffuse (81–100% of all tumor cells), *F* focal (11–50%), *M* moderate, *N* negative (<1%), *P* partial (51–80%), *R* rare (1–10%), *W* weak.
*Staining in mosaic pattern.

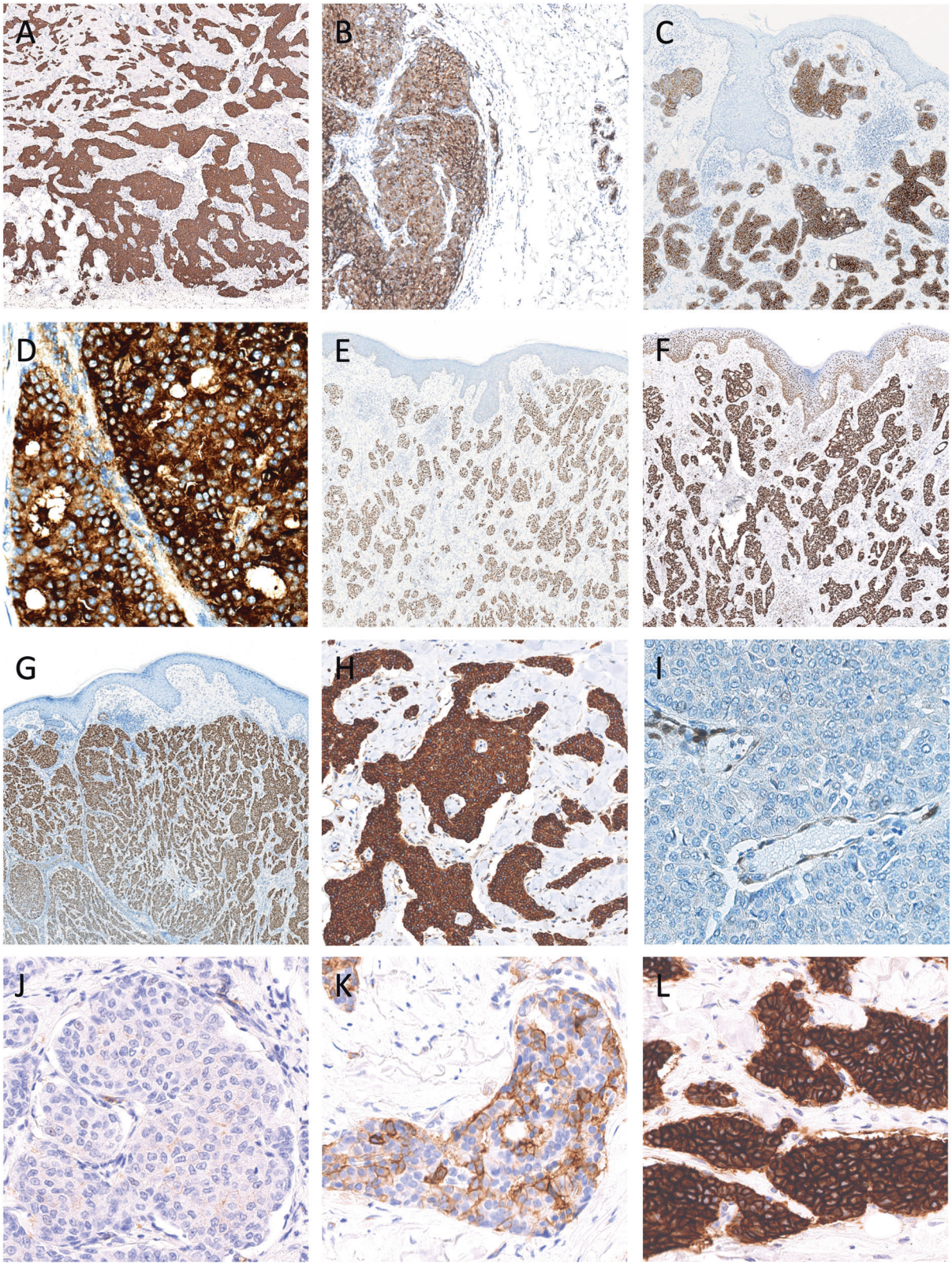

Fig. 5 Immunohistochemical findings of sweat-gland carcinoma with neuroendocrine differentiation (SCAND)/low-grade neuroendocrine carcinoma of the skin (LGNECS). Cytokeratin 19 (**A**), epithelial membranous antigen (**B**), BerEP4 (**C**), carcinoembryonic antigen (**D**), insulinoma-associated protein 1 (**E**), GATA3 (**F**), estrogen receptor (**G**), and bcl-2 (**H**) were diffusely positive in all evaluated cases. Complete loss of PTEN immunostaining was seen in case 7 and partial loss was in case 5 (**I**). The evaluation of somatostatin receptor subtype 2a staining revealed score 1 (**J**), score 2 (**K**), or score 3 (**L**).

Therefore, we propose a new name, "sweat-gland carcinoma with neuroendocrine differentiation" (SCAND) for LGNECS. All the tumors reported as LGNECS in previous papers[11–13] could be considered the same as SCAND. Further research with a larger sample size is required to confirm our findings.

REFERENCES

1. Busam K. J., Walsh N., Wood B. A. Merkel cell carcinoma. in (eds Elder, D. E., Massi, D., Scolyer, R. A., Willemze, R.) *WHO Classification of Skin Tumours*. 48–50 (IARC Press, 2018).
2. Albores-Saavedra, J. et al. Merkel cell carcinoma demographics, morphology, and survival based on 3870 cases: a population based study. *J. Cutan. Pathol.* **37**, 20–27 (2010).
3. Harms, K. L. et al. Analysis of prognostic factors from 9387 Merkel cell carcinoma cases forms the basis for the new 8th edition AJCC Staging System. *Ann. Surg. Oncol.* **23**, 3564–3571 (2016).
4. Flieder, A., Koerner, F. C., Pilch, B. Z. & Maluf, H. M. Endocrine mucin-producing sweat gland carcinoma: a cutaneous neoplasm analogous to solid papillary carcinoma of breast. *Am. J. Surg. Pathol.* **21**, 1501–1506 (1997).
5. Zembowicz, A. et al. Endocrine mucin-producing sweat gland carcinoma: twelve new cases suggest that it is a precursor of some invasive mucinous carcinomas. *Am. J. Surg. Pathol.* **29**, 1330–1339 (2005).
6. Tsai, J. H., Hsiao, T. L., Chen, Y. Y., Hsiao, C. H. & Liau, J. Y. Endocrine mucin-producing sweat gland carcinoma occurring on extra-facial site: a case report. *J. Cutan. Pathol.* **41**, 544–547 (2015).
7. Fernandez-Flores, A. Considerations before accepting an extra-facial location of endocrine mucin-producing sweat gland carcinoma. *J. Cutan. Pathol.* **42**, 297–298 (2015).
8. Held, L. et al. Endocrine mucin-producing sweat gland carcinoma: a clinicopathologic, immunohistochemical, and molecular analysis of 11 cases with emphasis on MYB immunoexpression. *J. Cutan. Pathol.* **45**, 674–680 (2018).
9. Qin, H. et al. Endocrine mucin-producing sweat gland carcinoma: a study of 11 cases with molecular analysis. *J. Cutan. Pathol.* **45**, 681–687 (2018).
10. Agni, M. et al. An update on endocrine mucin-producing sweat gland carcinoma: clinicopathologic study of 63 cases and comparative analysis. *Am. J. Surg. Pathol.* **44**, 1005–1016 (2020).
11. Goto, K. et al. Low-grade neuroendocrine carcinoma of the skin (primary cutaneous carcinoid tumor) as a distinctive entity of cutaneous neuroendocrine tumors: a clinicopathologic study of 3 cases with literature review. *Am. J. Dermatopathol.* **39**, 250–258 (2017).
12. Chen, T. Y., Morrison, A. O., Susa, J. & Cockerell, C. J. Primary low-grade neuroendocrine carcinoma of the skin: an exceedingly rare entity. *J. Cutan. Pathol.* **44**, 978–981 (2017).
13. Okabayashi, A., Nakagawa, K., Shimizu, N., Tohda-Kinoshita, R. & Goto, K. Case of low-grade neuroendocrine carcinoma of the skin presenting metastases to lymph nodes and peritoneum. *J. Dermatol.* **46**, 720–723 (2019).
14. Volante, M. et al. Somatostatin receptor type 2A immunohistochemistry in neuroendocrine tumors: a proposal of scoring system correlated with somatostatin receptor scintigraphy. *Mod. Pathol.* **20**, 1172–1182 (2007).
15. Karczewski, K. J. et al. The mutational constraint spectrum quantified from variation in 141,456 humans. *Nature* **581**, 434–443 (2020).
16. Auton, A. et al. A global reference for human genetic variation. *Nature* **526**, 68–74 (2015).
17. Tadaka, S. et al. jMorp: Japanese multi omics reference panel. *Nucleic Acids Res.* **46**, D551–D557 (2018).
18. Higasa, K. et al. Human genetic variation database, a reference database of genetic variations in the Japanese population. *J. Hum. Genet.* **61**, 547–553 (2016).
19. Wang, K., Li, M. & Hakonarson, H. ANNOVAR: Functional annotation of genetic variants from high-throughput sequencing data. *Nucleic Acids Res.* **38**, e164 (2010).
20. Dijk, C. V., Ten & Seldam, R. E. A possible primary cutaneous carcinoid. *Cancer* **36**, 1016–1020 (1975).
21. Nishimoto, M., Nanba, K., Itagaki, T. & Uemura, A. Primary cutaneous carcinoid in umbilicus [in Japanese]. *Jpn. J. Clin. Dermatol.* **38**, 471–476 (1984).
22. Smith, P. A. & Chappell, R. H. Another possible primary carcinoid tumour of skin? *Virchows Arch. A Pathol. Anat. Histopathol.* **408**, 99–103 (1985).
23. Collina, G., Quarto, F. & Eusebi, V. Trabecular carcinoid of the skin with cellular stroma. *Am. J. Dermatopathol.* **10**, 430–435 (1988).
24. Bart, R. S., Kamino, H., Waisman, J., Lindner, A. & Colen, S. Carcinoid tumor of skin: report of a possible primary case. *J. Am. Acad. Dermatol.* **22**, 366–370 (1990).
25. Sakamoto, F., Ito, M., Matumura, G., Sato, Y. & Kimura, S. Ultrastructural study of a mucinous carcinoid of the skin. *J. Cutan. Pathol.* **18**, 128–133 (1991).
26. Curville, P. et al. Primary cutaneous carcinoid tumour. *Histopathology* **36**, 566–567 (2000).
27. MacKenzie, D. N., McCormick, C. S. F. & Morris, R. J. Lymph node metastasis from a primary skin carcinoid tumour. *Br. J. Plast. Surg.* **56**, 718–721 (2003).
28. Cokonis, C. D., Green, J. J. & Manders, S. M. Primary carcinoid tumor of the skin. *J. Am. Acad. Dermatol.* **51**, S74–S76 (2004).
29. Eloy-Garcia Carrasco, C., Benguigui Benadiva, J., Martinez Garcia, S., Sanz Trelles, A. & Palacios, S. Atypical primary carcinoid tumour of the skin. *J. Cutan. Pathol.* **33** (suppl 2), 32–34 (2006).
30. Kropinak, M., Sims, L., Iacob, C., McCormick, S. A. & Milman, T. Primary typical carcinoid tumor of the eyelid. *Ophthal. Plast. Reconstr. Surg.* **25**, 318–320 (2009).
31. Terada, T. Primary cutaneous neuroendocrine tumor (atypical carcinoid) expressing KIT and PDGFRA with myoepithelial differentiation: a case report with immunohistochemical and molecular genetic study. *Int. J. Clin. Exp. Pathol.* **6**, 802–809 (2013).
32. Panse, G., Cowper, S. E., Leffell, D. J., Pulitzer, M. & Ko, C. J. Well-differentiated neuroendocrine tumors in skin: terminology and diagnostic utility of cytokeratin 5/6 and p63. *J. Cutan. Pathol.* **44**, 557–562 (2017).
33. Fernandez-Flores, A. Cutaneous metastases: a study of 78 biopsies from 69 patients. *Am. J. Dermatopathol.* **32**, 222–239 (2010).
34. Jedrych, J., Busam, K., Klimstra, D. S. & Pulitzer, M. Cutaneous metastases as an initial manifestation of visceral well-differentiated neuroendocrine tumor: a report of four cases and a review of literature. *J. Cutan. Pathol.* **41**, 113–122 (2014).
35. Chen, P. P. et al. High-grade neuroendocrine carcinomas of the vulva: a clinicopathologic study of 16 cases. *Am. J. Surg. Pathol.* **45**, 304–316 (2021).
36. The WHO Classification of Tumours Editorial Board (eds). *WHO Classification of Tumours.Digestive System Tumours* 5th edn. (IARC Press, 2019).
37. Soga, J. & Tazawa, K. Pathologic analysis of carcinoids. Histologic reevaluation 62 cases. *Cancer* **28**, 990–998 (1971).
38. Worby, C. A. & Dixon, J. E. PTEN. *Annu. Rev. Biochem.* **83**, 641–669 (2014).
39. Li, J. et al. PTEN, a putative protein tyrosine phosphatase gene mutated in human brain, breast, prostate cancer. *Science* **275**, 1943–1947 (1997).
40. Langer, S. W. et al. Cowden syndrome and concomitant pulmonary neuroendocrine tumor: a presentation of two cases. *Case Rep. Med.* **2015**, 265786 (2015).
41. Tsunezuka, H., Abe, K., Shimada, J. & Inoue, M. Pulmonary atypical carcinoid in a patient with Cowden syndrome. *Interact. Cardiovasc. Thorac. Surg.* **22**, 860–862 (2016).
42. Gong, J. et al. Multiplatform profiling of pancreatic neuroendocrine tumors: correlative analyses of clinicopathologic factors and identification of co-occurring pathogenic alterations. *Oncotarget* **10**, 6260–6268 (2019).
43. Chen, L. et al. Genetic characteristics of colorectal neuroendocrine carcinoma: more similar to colorectal adenocarcinoma. *Clin. Colorectal. Cancer* **20**, 177–185 (2021).
44. Ishida, S. et al. Neuroendocrine carcinoma and mixed neuroendocrine-non-neuroendocrine neoplasm of the stomach: a clinicopathological and exome sequencing study. *Hum. Pathol.* **110**, 1–10 (2021).
45. Cimic, A. et al. Molecular profiling reveals limited targetable biomarkers in neuroendocrine carcinoma of the cervix. *Appl. Immunohistochem. Mol. Morphol.* **29**, 299–304 (2021).
46. Bishop, J. A., Alaggio, R., Zhang, L., Seethala, R. R. & Antonescu, C. R. Adamantinoma-like Ewing family tumors of the head and neck: a pitfall in the differential diagnosis of basaloid and myoepithelial carcinomas. *Am. J. Surg. Pathol.* **39**, 1267–1274 (2015).
47. Goto, K. Immunohistochemistry for CD117 (KIT) is effective in distinguishing cutaneous adnexal tumors with apocrine/eccrine or sebaceous differentiation from other epithelial tumors of the skin. *J. Cutan. Pathol.* **42**, 480–488 (2015).
48. Nishida, H. et al. KIT (CD117) expression in benign and malignant sweat gland tumors. *Am. J. Dermatopathol.* **37**, 898–905 (2015).
49. Goto, K. et al. CD117 (KIT) is a useful immunohistochemical marker for differentiating porocarcinoma from squamous cell carcinoma. *J. Cutan. Pathol.* **43**, 219–226 (2016).
50. Sugita, K., Yamamoto, O., Hamada, T., Hisaoka, M. & Tokura, Y. Primary apocrine adenocarcinoma with neuroendocrine differentiation occurring on the pubic skin. *Br. J. Dermatol.* **150**, 371–373 (2004).
51. Li, Y., Chen, L. I., Li, B., Tian, X. & Li, Z. Unusual apocrine carcinoma with neuroendocrine differentiation: a cutaneous neoplasm may be analogous to neuroendocrine carcinoma with apocrine differentiation of breast. *Diagn. Pathol.* **10**, 64 (2015).
52. Imamura, T., Kuwahara, F., Saruta, H., Nakama, T. & Ohata, C. Apocrine carcinoma with neuroendocrine differentiation. *J. Cutan. Pathol.* **44**, 810–812 (2017).

ACKNOWLEDGEMENTS

The authors thank Ms. Fujiko Ishimoto and Mr. Kikuichi Nakagawa for their superb technique.

AUTHOR CONTRIBUTIONS

K.G. designed the study, analysed the clinicopathologic data, and wrote and edited the paper. Y.K. analyzed the molecular data of the samples. All authors provided the cases, extracted the clinical data, reviewed the paper, and gave the final approval for publication.

FUNDING

Supported in part by OICI fund for Department of Dermatologic Oncology in 2020.

COMPETING INTERESTS

The authors declare no competing interests.

ETHICS APPROVAL

The study was conducted according to the Declaration of Helsinki and has been approved by the research ethics committee of the Osaka International Cancer Institute, Osaka, Japan (reference number: 20113).

ADDITIONAL INFORMATION

Correspondence and requests for materials should be addressed to Keisuke Goto.